8-11 JULY 2024 ICSV30 AMSTERDAM

ASSESSMENT OF SOUND INSULATION FOR INNOVATIVE ULTRA-HIGH-PERFORMANCE CONCRETE CORE THERMAL BREAKS

Tran-Van Han[a,b,*], Gayoon Lee[a], Nguyen Huu Cuong[a,c] and Kihak Lee[a]

[a]*Deep Learning Architecture Research Center, Department of Architectural Engineering, Sejong University, 209 Neungdong-ro, Gwangjin-gu, Seoul 05006, Republic of Korea.*

[b]*Faculty of Civil Engineering, Mien Trung University of Civil Engineering, Tuy Hoa and Danang, Viet Nam.*

[c]*Department of Civil Engineering, Vinh University, Vinh 461010, Viet Nam*

[*] *E-mail: tranhan1405@gmail.com*

This study examines the acoustic performance of a novel thermal break featuring Ultra-High-Performance Concrete (UHPC) cores and thermal insulation layers, aimed at reducing heat loss at building wall junctions. By adjusting the thicknesses of expanded polystyrene (EPS), cellulose fiber reinforced cement board (CRC), and Melamine foam, it identifies optimal configurations for enhanced sound insulation. Key findings from the tests suggest that reducing the thickness of EPS while incorporating thicker CRC layers, and increasing the thickness of Melamine foam, significantly improves the sound insulation performance. Additionally, a numerical analysis was conducted and validated by experimental data, emphasizing the critical impact of material selection on the sound insulation efficacy of the novel thermal break.

Keywords: Thermal bridges, Thermal break, Airborne sound insulation, Acoustic insulation, Wall intersection.

1. Introduction

Energy consumption in the building sector represents 40% of global use, increasing rapidly due to higher heating and cooling demands and contributing significantly to carbon emissions [1]. This issue is particularly pronounced in Korea, where extreme seasonal temperature variations lead to substantial energy use. Facades, being a primary source of energy loss, account for over half of a building's energy demand [2].

Thermal bridges [3] at structural junctions significantly undermine building thermal performance, leading to increased heat loss in winter and heat gain in summer. These bridges, either linear or punctual, exacerbate energy inefficiency, especially with the common use of internal insulation in multi-residential buildings, which is often disrupted at structural joints. This not only increases energy consumption but also risks condensation, mold growth, and reduced indoor air quality.

Addressing thermal bridges is crucial for energy efficiency and a healthy indoor environment. Research has shown that implementing thermal breaks in balcony structures can decrease heat transfer by

72% to 85% [4], significantly improving interior temperatures. However, studies on reducing thermal bridges through wall connections are limited.

Cuong et al. [5] developed a vertical thermal bridge break for the interface between outer and inner walls, featuring a low thermal conductivity break that hinders heat transfer, stabilized by a core made of UHPC and insulated with thermal layers. This innovation not only reduces thermal bridging but also maintains structural integrity and enhances energy efficiency.

While much research has focused on thermal insulation effectiveness, the sound insulation capabilities of thermal breaks are often overlooked. Indoor noise transmission through walls, with thermal breaks being notable weak points, significantly impacts building acoustic environments. This research investigates the airborne sound insulation performance of thermal breaks in wall connections, aiming to enhance both energy efficiency and acoustic comfort in buildings.

The paper is structured to detail the experimental programs and acoustic numerical analysis, discuss results, and conclude with key findings, offering insights into the acoustic design and construction of the innovative thermal break in building structures.

2. The concept of the novel UHPC core thermal break at the wall intersection

The concept of this thermal break at the wall intersection is illustrated in Fig.1a. Central to this system is a connector core made of UHPC, reinforced with stainless steel bars and insulated with thermal layers. The actual image of the thermal break is shown in Fig.1b. UHPC cores and stirrups are utilized to connect and secure the outer and inner walls of the building, as depicted in Fig. 1c. This design not only establishes a thermal break but also maintains the structural integrity of the building's reinforced concrete framework.

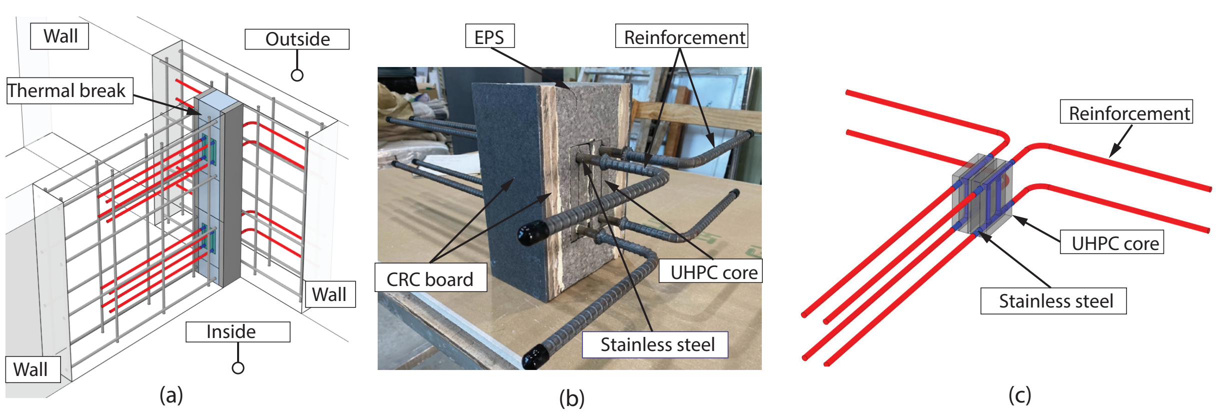

Figure 1: The concept of the thermal break at the wall intersection [5]: (a) Thermal break inside the building; (b) The actual image of the thermal break; and (c) the core of a thermal break.

3. Experimental program

In this study, the thermal break's design specimen includes a variety of insulating materials but omits the UHPC core for the experimental focus. The assembly features three insulation types: CRC board, EPS, and Melamine foam (referred to as M), with respective densities of 1400, 31, and 9 kg/m^3. Of these, CRC board and EPS have Young's moduli of 15000 MPa and 8 MPa, respectively. The properties of these materials are detailed in Table 1. The acoustic properties of Melamine, which depend on its thickness, are depicted in Fig. 2.

Table 1: Mechanical properties of the specimens

No.	Material	Young's modulus (MPa)	Poisson's ratio	Compressive strength (MPa)	Mass density (kg/m^3)
1	CRC	15000	0.16	18.6	1400
2	EPS	8	0.3	0.27	31
3	Melamine	-	-	-	9

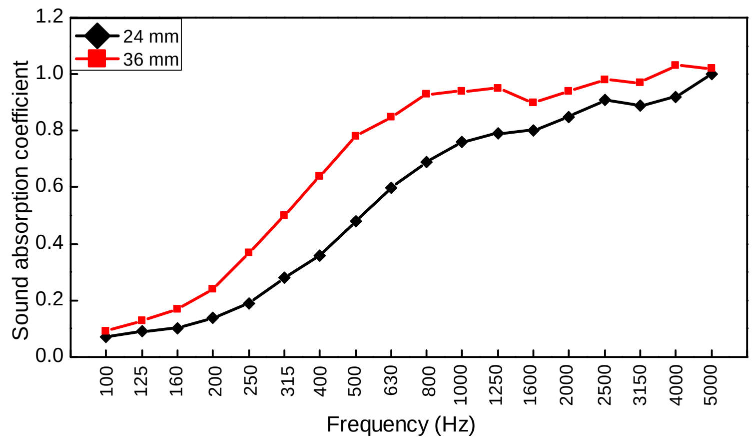

Figure 2: Dependence of sound absorption coefficient on thickness for melamine.

The study assessed three configurations of thermal break for comparative analysis. Each assembly was characterized by a uniform thickness of 200mm and was evaluated across a surface area dimensions 1480×225 mm^2, corresponding to height and width, respectively. The test specimens varied in terms of material compositions, and surface densities, with specifics enumerated in Table 2. The configurations, identified by their composite materials CRC12/ CRC12/ EPS152, CRC6/ CRC12/ CRC12/ EPS140, and CRC12/ M12/ CRC6/ EPS140 exhibited surface densities of 359.56, 441.7, and 274.78 kg/m^2, respectively.

Table 2: Configurations for the novel thermal break specimens

Test	Wall type	Thickness (mm)	Height (mm)	Width (mm)	Area (m2)	Surface Density (kg/m^2)
1	CRC12/CRC12/EPS152	200	1480	225	0.33	359.56
	CRC6/CRC12/CRC12/EPS140	200				441.7
	CRC12/M18/EPS140	200				191.32

Sound insulation tests were conducted following ISO 10140-2:2021, using white noise to measure sound pressure levels (SPL) in source and receiving rooms. SPLs were averaged in 1/3 octave bands and integrated over time and space to calculate the sound reduction index (R), per ISO 717-1 [6]. This index assesses frequency-dependent sound isolation, further distilled into the Weighted Sound Insulation Index (R_w) for easier comparison of building elements. Correction terms for traffic (C_{tr}) and pink noise (C) were also determined to evaluate insulation effectiveness against various noises.

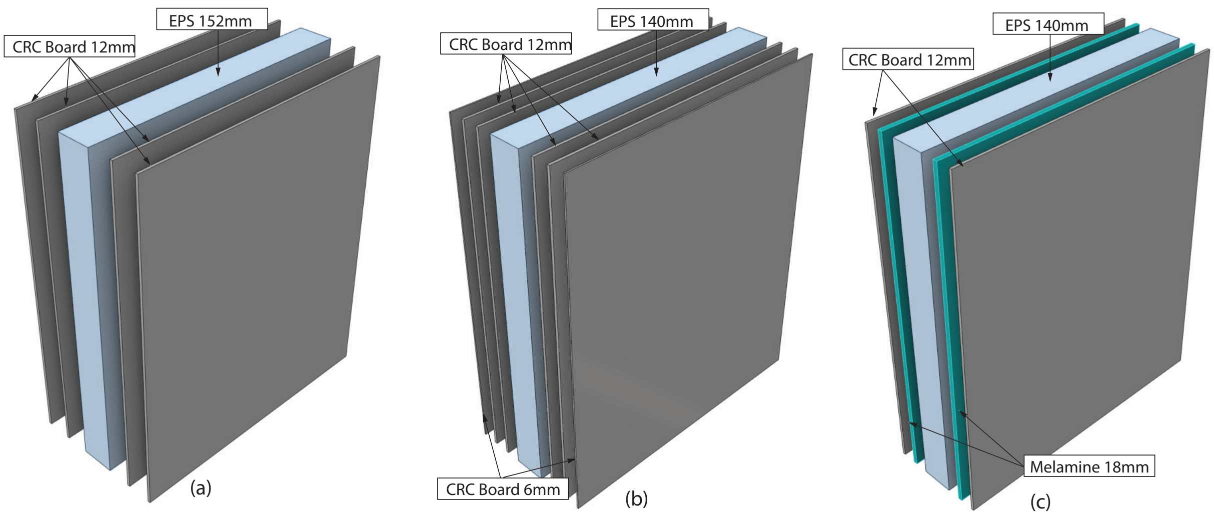

Figure 3: Composition of the specimens:(a) CRC12/ CRC12/ EPS152;(b) CRC6/ CRC12/ CRC12/ EPS140; and (c) CRC12/M18/EPS140).

The R value is given by:

$$R = L_1 - L_2 + 10 \log \left(\frac{S}{A} \right) \tag{1}$$

where L_1 and L_2 are the average SPLs in the source and receiving rooms, respectively, S is the tested module's surface area, and A, the sound absorption area in the receiving room, is calculated as:

$$A = \frac{0.163 \times V}{T} \tag{2}$$

Here, V is the room volume, and T is the reverberation time, determined from six measurements without background noise correction, using averaged decay signals between -5 and -25 dB.

Fig. 4 shows the arrangement of the experimental instruments used to measure sound insulation performance in the ISO-compliant reverberation room.

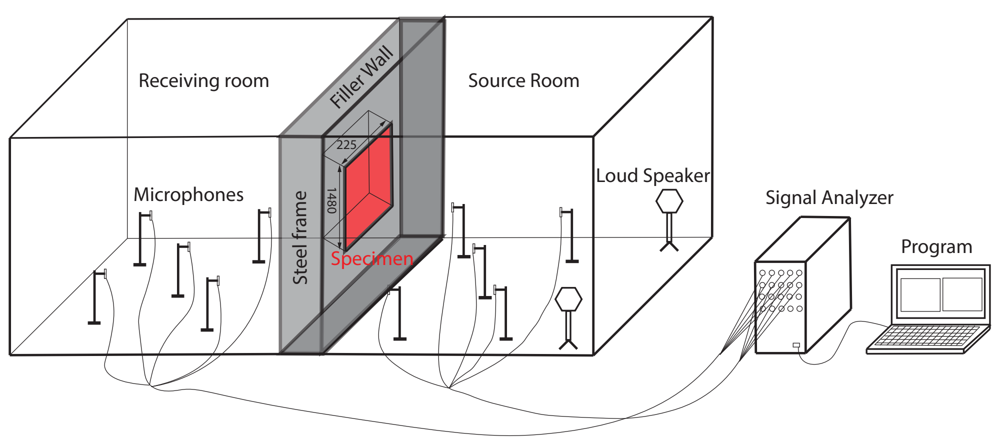

Figure 4: Experimental instrument setup.

4. Experimental results and discussion

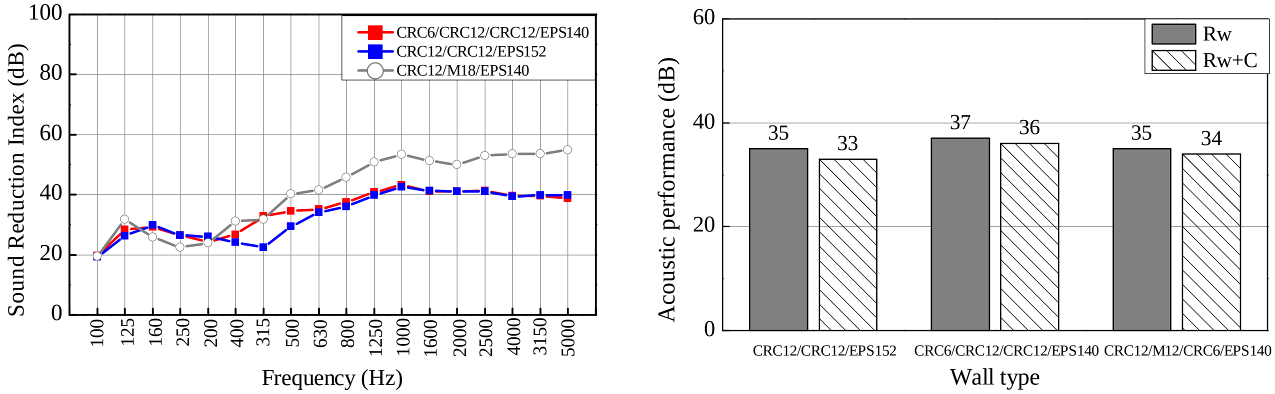

(a) Sound reduction index.

(b) Overall acoustic performance.

Figure 5: The acoustic performance of the specimens.

The graphical representation of the sound reduction index's frequency dependence, within the 100–5000 Hz range, is depicted Fig. 5(a).

- For specimens without Melamine (CRC12/CRC12/EPS152 and CRC6/CRC12/CRC12/EPS140):
  - In the stiffness-controlled region (below 250 Hz), negligible changes in sound insulation were observed. The CRC6/CRC12/CRC12 specimen showed a transmission loss up to 2.2 dB higher at 125 Hz than CRC12/CRC12/EPS152, indicating a marginal increase in stiffness due to a 12 mm reduction in EPS thickness and the addition of a 12 mm CRC layer.
  - In the mass-controlled region (250 Hz to 1250 Hz), the CRC6/CRC12/CRC12/EPS140 specimen exhibited superior insulation, especially between 315-500 Hz, with transmission loss values 2.6, 10.5, and 5.2 dB higher at the respective frequencies. This improvement is attributed to the increased mass from an additional CRC board layer and reduced EPS thickness. Changes beyond 500 Hz were minimal.
  - In the damping-controlled region (1250 Hz to 5000 Hz), no significant changes in insulation capabilities were noted, with the largest difference being 1.0 dB at 5000 Hz. This suggests that material alterations do not significantly influence insulation at higher frequencies due to the limited damping properties of CRC and EPS.
- For the CRC6/CRC12/CRC12/EPS140 specimens, comprising CRC board and EPS, and the CRC12/ M18/ EPS140 specimen, created by substituting CRC board with a Melamine foam layer of identical thickness (36 mm), sound performance comparisons revealed:
  - In the stiffness-controlled region (100-250 Hz), CRC6/CRC12/CRC12/EPS140 generally exhibited superior sound insulation capabilities over CRC12/M18/EPS140, especially at 200 Hz where it demonstrated a 4.1 dB higher sound insulation. This is attributed to the higher stiffness of CRC compared to Melamine foam of the same thickness.
  - Within the mass-controlled region (250-1250 Hz), the CRC12/M18/EPS140 specimen outperformed CRC6/CRC12/CRC12/EPS140, with transmission loss values ranging from 4.5 to 10.2 dB higher. This superior performance is due to the higher sound absorption coefficient of Melamine foam.
  - In the damping-controlled region (1250-5000 Hz), a significant difference was observed, with CRC6/CRC12/CRC12/EPS140 showing considerably worse acoustic performance compared to CRC12/M18/EPS140, with differences in transmission loss values ranging from 10.3

to 16.1 dB. This indicates that Melamine foam's damping properties substantially improve sound insulation at higher frequencies.

Fig. 5(b) present the overall sound insulation performances of the experimental specimens.

- The CRC6/CRC12/CRC12/EPS140 specimens exhibited superior sound insulation, with R_w and $R_w + C$ values increasing by 2-3 dB compared to CRC12/CRC12/EPS152. This improvement is attributed to increased surface mass and stiffness, achieved by reducing EPS thickness by 12 mm and adding an additional 12 mm CRC layer. These results suggest that enhancing mass and stiffness can significantly improve the acoustic performance of the novel thermal break.
- In comparison, CRC12/M18/EPS140 outperformed CRC6/CRC12/CRC12/EPS140, demonstrating a 2-3 dB increase in R_w and $R_w + C$ values. The enhanced sound insulation at lower frequencies provided by the greater stiffness and mass of CRC6/CRC12/CRC12/EPS140 contrasts with CRC12/M18/EPS140's superior sound absorption capabilities at higher frequencies.
- Among the tested specimens, CRC12/M18/EPS140, with its Melamine foam layer, marked the most pronounced improvement in sound insulation, showing a 2-5 dB enhancement over specimens without Melamine. This underscores Melamine's effectiveness as a soundproofing material for the novel thermal break.

5. Finite element modeling

5.1 Numerical modeling

To investigate the acoustic performance of innovative UHPC concrete core thermal breaks, a numerical model was developed using Simcenter 3D version 2021.2, a SIEMENS product. Employing the finite element (FE) method, this model aimed to replicate the experimental setup previously described, specifically focusing on the CRC12/M18/EPS140 specimen. As shown in Fig. 6a, the model includes 3D elements to simulate the air within both the source and receiving rooms (Acoustic fluid elements-CTETRA), in addition to the specimen's CRC, Melamine, and EPS layers (CHEXA8 elements).

Mechanical properties and geometric parameters of the specimen CRC12/M18/EPS140 were calibrated to match those of the experimental mock-up. Air was modeled with a density of 1.2 kg/m^3 and a sound speed of 340 m/s, reflecting actual conditions. It is noted that the Melamine insulation property was simulated using an impedance coefficient, which was calculated based on the sound absorption coefficients depicted in Fig. 2.

$$\alpha = \frac{4Z_R}{\rho c}\left[\left(1+\frac{Z_R}{\rho c}\right)^2+\left(\frac{Z_I}{\rho c}\right)^2\right]^{-1} \tag{3}$$

Where Z is the impedance coefficient, Z_R the real part, and Z_I the imaginary part; α the acoustic absorption coefficient; ρ the air density, and c the speed of sound in air.

Simcenter 3D streamlines the modeling of source and receiving rooms by simulating only the air contained within, enhancing the analysis process. For accurate emulation of non-reflective acoustic boundary conditions, Automatically Matched Layers (AML) [7] were applied to the air surfaces of both rooms, as depicted in Fig. 6b, demonstrating the boundary conditions implemented in this model.

5.2 Verification of the FE model

Fig. 7 illustrates the comparison of the sound reduction index across 1/3 octave bands, derived from both field measurement and numerical simulation. The numerical models demonstrated a high degree of precision in predicting the sound reduction index, with the maximum discrepancy reaching 13.01%

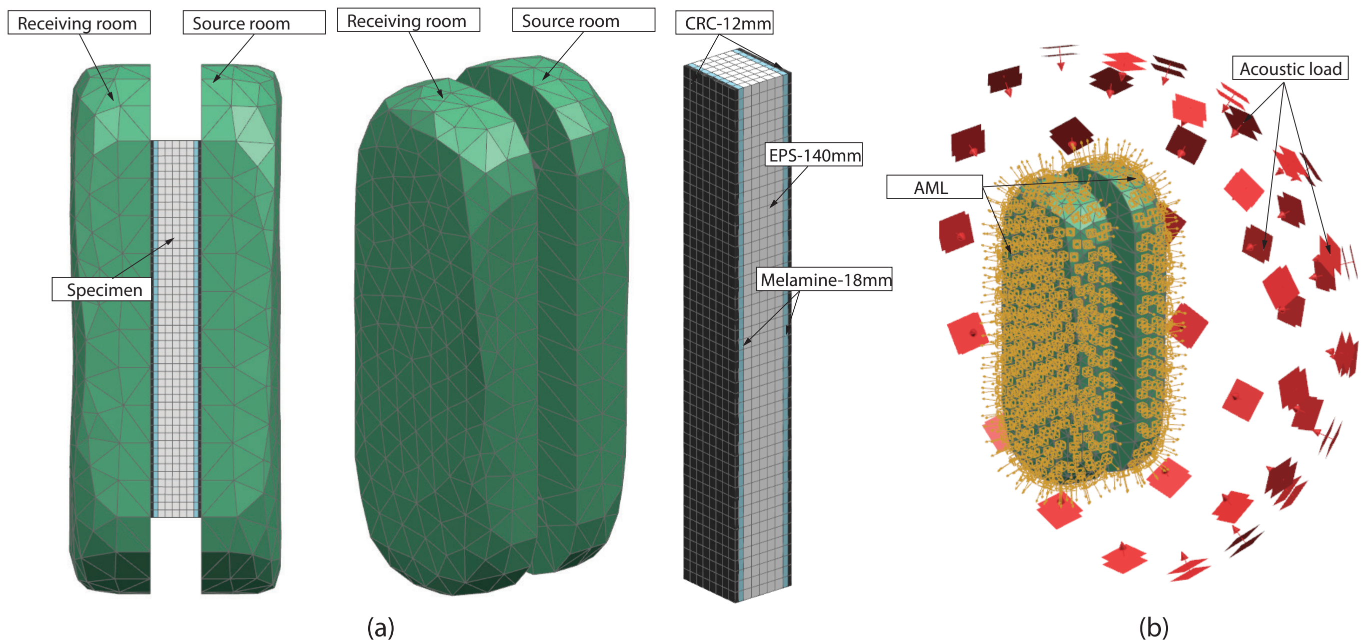

Figure 6: Details of FE models used for numerical investigation: (a) FE model; (b) boundary conditions with Automatically Matched Layers (AML).

at 100Hz. This close alignment between the experimental data and simulation outcomes across the frequency spectrum emphasizes the effectiveness of the finite element method in accurately forecasting acoustic performance. Consequently, this approach allows for a comprehensive parametric analysis, offering a viable substitute for labor-intensive and financially demanding field measurements.

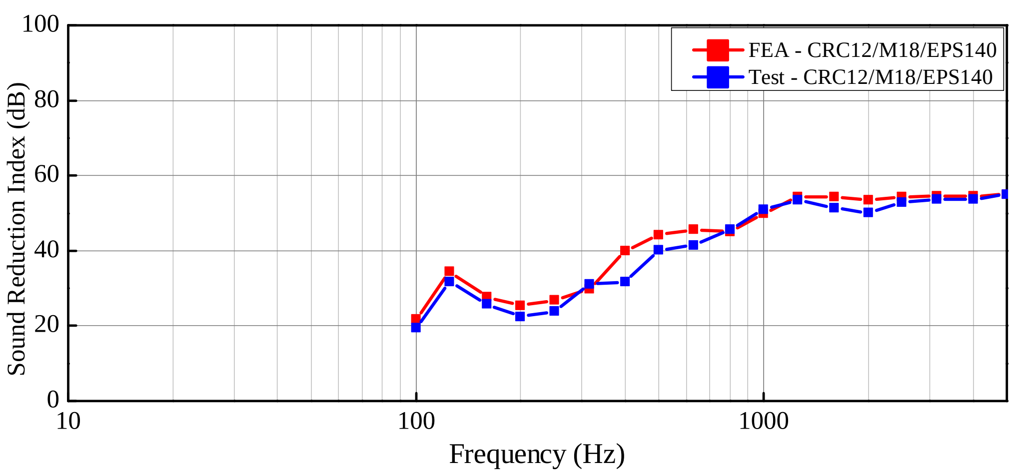

Figure 7: Comparison of experimental and numerical results of the CRC12/M18/EPS140 specimen.

6. Conclusions

The experimental and numerical analysis of various wall specimens in this study underscores the significant impact of material composition and structure on sound insulation effectiveness. Key observations include:

- Adjusting the material layers of EPS and CRC significantly influences the acoustic performance of the novel thermal break. Specifically, experimental results indicate that increasing the mass and stiffness—by reducing the EPS thickness by 12 mm and adding an additional CRC layer of the same thickness—resulted in a notable improvement of 2-3 dB in sound insulation performance.
- Melamine has been shown to be an effective material for soundproofing for the novel thermal breaks. Experimental results demonstrate that the most significant increase in sound insulation, with a 2-5 dB enhancement, was observed in specimens with the thickest Melamine layer. This highlights the direct relationship between material thickness and insulation efficiency, especially for Melamine foam.
- The acoustic performance prediction for the innovative UHPC concrete core thermal breaks was validated using commercial software by comparing field measurements with the numerical model across a one-third octave frequency range. This comparison confirmed the accuracy of the acoustic analysis.
- It is proposed that numerical simulations, as demonstrated, could effectively replace the need for more costly and time-consuming field experiments.

7. Acknowledgments

This research was supported by Basic Science Research Program through the National Research Foundation of Korea(NRF) funded by the Ministry of Education(RS-2023-00247959).

REFERENCES

1. Harish, V. and Kumar, A. A review on modeling and simulation of building energy systems, *Renewable and sustainable energy reviews*, **56**, 1272–1292, (2016).

2. Ascione, F., Bianco, N., Mauro, G. M. and Napolitano, D. F. Building envelope design: Multi-objective optimization to minimize energy consumption, global cost and thermal discomfort. application to different italian climatic zones, *Energy*, **174**, 359–374, (2019).

3. ISO, E. 10211:2017: Thermal bridges in building construction-heat flows and surface temperaturess, *International Organization for Standardization, Geneva*, (2017).

4. Ge, H., McClung, V. R. and Zhang, S. Impact of balcony thermal bridges on the overall thermal performance of multi-unit residential buildings: A case study, *Energy and Buildings*, **60**, 163–173, (2013).

5. Cuong, N. H., Gayoon, L., An, H., An, S., Han, S. W. and Lee, K. Experimental evaluation of a vertical heat bridge insulation system for the structural performance of multi-residential buildings, *Structures*, vol. 58, p. 105686, Elsevier, (2023).

6. ISO, I. 717-1; acoustics—rating of sound insulation in buildings and of building elements—part 1: Airborne sound insulation, *International Organization for Standardization: Geneva, Switzerland*, (2013).

7. SIEMENS, *Acoustics User's Guide*, Siemens Product Lifecycle Management Software Inc. (2016).